Available online at www.sciencedirect.com

ScienceDirect

Transportation Research Procedia 00 (2022) 000–000

Transportation Research Procedia

www.elsevier.com/locate/procedia

Transport Research Arena (TRA) Conference

Integrating social vulnerability into climate adaptation of urban transport in Maputo, Mozambique

M. Loli[a]*, G. Kefalas[b], E. Bouzoni[c], G. Diaz Fanas[e], S.A. Mitoulis[a], L. Kapetas[d], and F. Arroyo Arroyo[e],

[a]*University of Surrey, Stag Hill, Guildford GU2 7XH, UK*
[b] *International Hellenic University, 14th km Thessaloniki, Nea Moudania, Greece*
[c]*Grid Engineers, Pampouki 3, Athens 15451, Greece*
[d]*Stichting Global Resilient Cities Network, Korte Hoogstraat 3, 3011 GK Rotterdam, The Netherlands,*
[e]*The World Bank, 1818 H St. NW, Washington, DC 20433, USA*

Abstract

Climate adaptation and risk reduction strategies in disaster-prone developing countries must be built on a sound understanding of the drivers of humanitarian risk. As part of a major urban mobility project planned by the Government of Mozambique (The World Bank, 2022), this study has mapped flood-prone areas in the Maputo Metropolitan Area based on a statistical analysis of the controlling geomorphological, meteorological, hydrological, and geographical factors, carried out in GIS. The exposure of the population was evaluated based on census data also considering the location of critical facilities. Socioeconomic parameters relevant to poverty and the presence of vulnerable groups have been considered for the estimation of human vulnerability. The reported risk analysis will be useful for an equity-centered prioritization of climate adaptation interventions in the existing network.

Peer-review under responsibility of the scientific committee of the Transport Research Arena (TRA) Conference
Keywords: natural hazards; urban mobility; climate adaptation; social inclusion; transport poverty;

1. Background

In Mozambique, extreme weather events have a measurable impact on social and economic growth. Triggered by cyclones and intense rain events, floods have become more frequent in recent years and are expected to follow this trend due to climate change. Recently, major floods following the passage of cyclones Idai and Kenneth (2019) caused 603 fatalities, leaving 1641 people injured and 2.5 million people in need of humanitarian aid, of which 1.3 million

* Corresponding author.
E-mail address: m.loli@surrey.ac.uk

Peer-review under responsibility of the scientific committee of the Transport Research Arena (TRA) Conference

were children. At the capital, Maputo, and the surrounding cities and districts (Matola, Marracuene, and Boane) that form the Greater Maputo Area (GMA) accessibility to jobs, health, and education facilities for the poorest population is one of the lowest in Africa, with one-third of public transport users reporting that flooding hinders their access to jobs during rainy days.

Nomenclature

d_H	Distance from hospitals
d_S	Distance from schools
E	Exposure
H	Hazard
L	Lack of coping capacity
P	Poverty
PMT	Proxy means testing
R	Risk
SSP	Shared Socioeconomic Pathways
V	Vulnerability

1.1. Study area

The Infulene river serves as the boundary between the municipalities of Maputo and Matola. Its drainage basin, (Fig. 1(a)), has an area of 302 km^2 and includes Maputo city, the capital, which is the country's political and industrial center. Mobility across the region is inadequate, sparse and of low reliability, due to the deficit road network. A significant proportion of roads in Maputo and Matola are unpaved and in poor condition. What is more, drainage infrastructure is scarce while the functionality of the very few roadside trenches is often compromised by debris blockages due to lack of maintenance. As a result, rainfall events lead to widespread flooding (Fig. 1(b) – (c)), causing severe disruptions due to the inundation of roads, even along primary roads and central arteries (Fig. 1(b)).

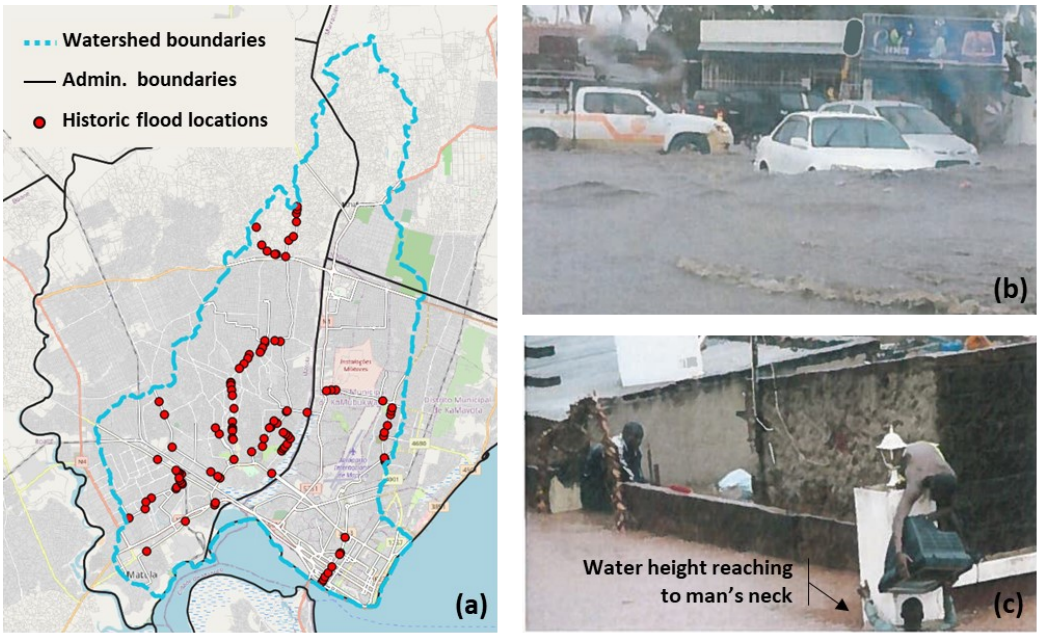

Fig. 1. (a) first picture; (b) second picture.

Based on interviews with over 200 residents and 100 frequent travelers carried out in 2015, the Municipality of Matola mapped flood susceptible locations in the region, especially focusing on mapping problematic sections of the road network (shown as points in Fig. 1(a)). Responses to questionnaires indicate that during the rainy season (October – March) flood induced travel disruptions become a routine. Many users reported that, in addition to being unable to use their old cars when streets are inundated, flooding also restricts their access to public transport. Certain parts of the network remain inundated for days, leading to sustained isolation of people, who report this as a significant obstruction of access to opportunities. Furthermore, the livability and safety of nearby residential houses deteriorate tremendously, as water remains inside houses and backyards for days (Fig. 1(c)).

2. Analysis in GIS

A variety of data layers were collected and analysed in GIS, according to the methodological flow-chart depicted in Fig. 2, exploiting remote sensed imagery and publicly available climate data, topography maps, street maps, as well as socioeconomic datasets provided by local authorities (e.g.: census, locations of critical facilities).

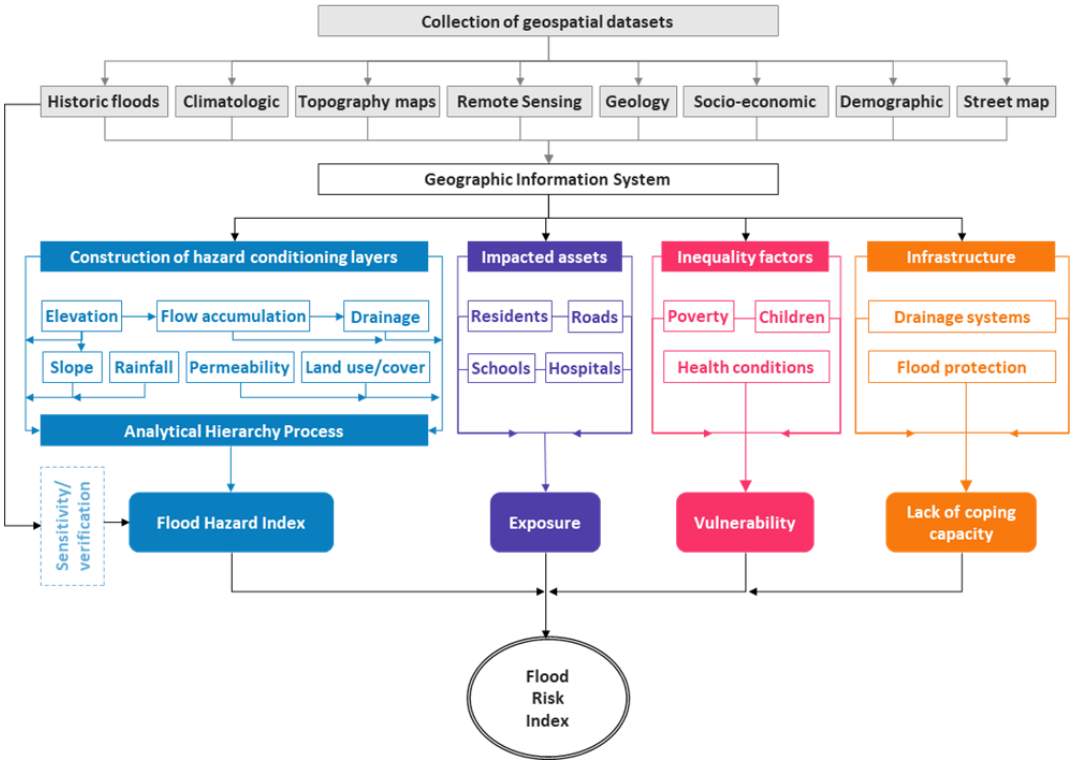

Fig. 2. Methodology: analysis of flood risk in GIS

2.1. Flood hazard index

Flood hazard assessment is the primary component of our approach to flood risk. Analysis at the watershed level by use of fluid mechanic modelling of floodplain inundation is a challenging and resource-demanding exercise (Bates, 2022). In recent years, statistical approaches to flood susceptibility have become an increasingly popular alternative (e.g.: Arabameri et al., 2019; Dodangeh et al., 2020; Lyu et al., 2018; Mahmoud & Gan, 2018; Phongsapan et al., 2019; Tang et al., 2018) due to their limited requirement for data, in comparison to conventional rainfall–runoff modelling methods, and ability to build upon public earth observation datasets to conduct the analysis at a regional scale. In this study, Flood Hazard Indexing (FHI) has been based on a Multi-Criteria Decision Analysis, implemented

in GIS, in conjunction with the Analytical Hierarchy Process, following Kazakis et al. (2015). This method has the advantage of being easily adjustable and tailored to the characteristics of the specific application.

FHI is here estimated based on seven conditioning parameters, namely: i) the ground elevation, which is derived using the latest global digital elevation model (Hawker et al., 2022); (ii) ground slope; (iii) flow accumulation, estimated using the channel network algorithm; (iv) land use/cover as observed by Sentinel 2 images; (v) distance from the drainage network/streams; (vi) geology; and (vii) rainfall.

Current (baseline) rainfall intensity is represented through averaging of wettest month precipitation from 1970 – 2000, as retrieved from WorldClim. Future climate is uncertain, yet projections show intensification of storm events over time. Climate change is considered in view of rainfall projections compatible with the Shared Socioeconomic Pathways (SSPs) framework, developed by O'Neill et al. (2016). Available through Phase 6 of the World Climate Research Program Coupled Model Intercomparison Project (CMIP6), the SSP framework contains multi-model climate projections based on five alternative/plausible scenarios of future emissions and land-use changes, by which society and ecosystems will evolve in the 21st century. We use a detrimental scenario (namely the SSP5-8.5) to highlight the likely dramatic increase of the region's flood susceptibility and the increasing urgency to adapt to climate impacts and build resilience for the communities.

The above (i) – (vii) parameter layers are synthesized, as described in Loli et al. (2022) who extended the work of Kapetas (2021) to create qualitative maps of flood susceptibility. As shown in Fig. 3, current (Fig 3(a)) and future (Fig. 3(b)) flood susceptibility is classified in five classes ranging from "very low" to "very high".

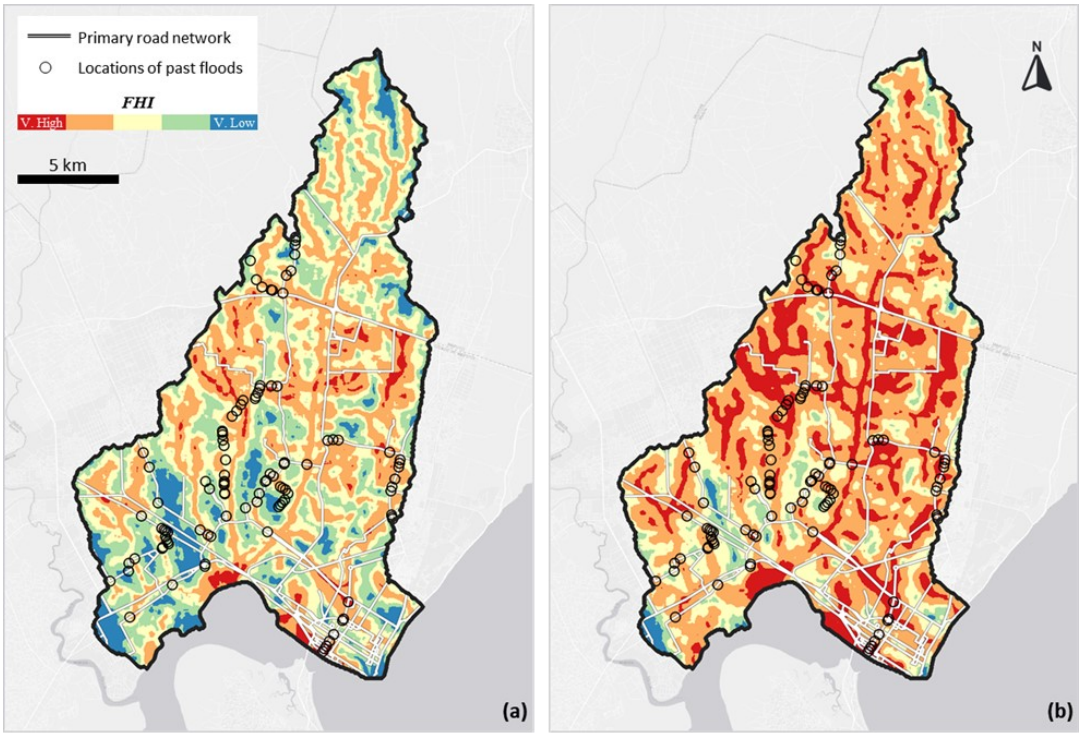

Fig. 3. FHI map of the Infulene catchment for the (a) baseline climate scenario and (b) for the 2021 – 2040 climate projection assuming the most pessimistic socioeconomic and climate predictions, as per the SSP5-8.5 scenario.

Fig. 3(a) shows the distribution of the FHI in GMA for the baseline climate scenario, achieving reasonably good agreement with empirical data. Observe that locations of predicted very high/high flood susceptibility are consistent with locations of reported flooding. It should be noted that the lack of historic flood evidence in regions where we predict high susceptibility is not a certain indicator of inaccurate prediction, due to possible under-reporting of flooding occurrences. Fig. 3(b) suggests a significant amplification of flood hazard up to 2040. This is the result of a

substantial rise in precipitation (about 20 mm on average for the wettest month), as predicted under the SSP5-8.5 scenario. For this rather pessimistic climate scenario, we predict a dramatic expansion of the highly susceptible areas while very few locations in GMA remain safe from flooding. Areas of low or medium flood hazard exposure today, appear to being shifted to higher hazard exposure in the future. As a result, GMA may see a dramatic rise in flooding in road segments that appear to be floodproof today.

2.2. Exposure of the road network

The primary and secondary road network (retrieved from OpenStreetMap via the OSMnx python package) is superimposed upon the FHI maps of Fig.2 to illustrate its exposure to flooding. Notably, only 30% of the over 340 km long road network crosses areas of very low to low flood susceptibility. By contrast, a very significant proportion of the network, estimated at 45% of its total length, is currently exposed to very high or high flood susceptibility. Calculations for SSP5-8.5 show that as much as 70% of the existing road network in GMA, i.e a threefold increase compared to current estimates, may be highly exposed to flooding in 18 years from now. This is a particularly alarming prediction calling for immediate investment to flood resilience and climate adaptation of the transport network as well as urban development in GMA.

2.3. Human vulnerability

Natural hazards impact disproportionately the most vulnerable populations and deepen social inequalities (Cremen et al., 2022; Wing et al., 2022). In Maputo, inequalities have a long history, originating from colonial times. Social division and polarization are evident in the census data shown in Fig. 4. As described in detail by Boyd et al. (2014), two urban nuclei co-exist in Maputo: the formerly “white” neighborhoods, downtown, where the estimated household income is relatively high; and the informal settlements on the outskirts of the city, which were initially established to accommodate the indigenous population and then, during the first decades of the twentieth century, received many immigrants from other parts of Africa and the Middle East. In addition to poverty, Maputo’s peri-urban communities suffer from a general lack of urban planning and construction standards, which further amplify their vulnerability to flooding.

Household income, as estimated via proxy means testing (PMT) carried out by the government and reported in Sohnesen et al., (2021), is here used as a determinant of social vulnerability. Poorer people tend to have less resilient dwellings, lesser financial resources to draw upon after a flood, greater professional insecurity, and reduced access to healthcare, all of which contribute to worse outcomes on the aftermath of a flood. Additional social and demographic factors can also influence vulnerability, including age, gender, health status, employment status etc. Exploiting the only relevant, available datasets, we consider the factor of age through consideration of the locations of schools (Fig. 5(a)), where children are naturally expected to concentrate. Furthermore, we use the location of hospitals to incorporate the vulnerability of groups that have underlying health conditions (Fig. 5(b)). Aggregation of vulnerable populations in these locations is considered by the introduction of high-vulnerability zones at a radius of 0.5 km from the center of schools and hospitals. In the respective layers (Fig. 5), vulnerability is assumed to decrease with spatial distance from the location of the critical facility. A radius of influence of 6 km is assumed to enclose every facility.

We create an integrated layer of social vulnerability (V) estimated as the resultant of the three components, namely poverty (P), distance from schools (d_S), and distance from health facilities (d_H):

$$V = \frac{1}{3}P + \frac{1}{3}d_S + \frac{1}{3}d_H \tag{1}$$

Flood risk (R) is analyzed following the INFORM methodology (Marin-Ferrer et al., 2017), a recently developed framework proposed by the UN for the evaluation of risk from natural and manmade hazards in regions where human vulnerability is significant, as is the case in GMA. As implied by the flowchart of Fig. 2, R is the resultant of four components: hazard (H), exposure (E), vulnerability, and the lack of coping capacity (L). While V considers the susceptibility of individuals and households, the component of coping capacity considers the dimension of institutional resources for alleviating disaster impacts. L encloses policies for disaster risk reduction and the presence and

functionality of basic infrastructure for response and recovery. Having no measurable information about *L* in GMA, at the district (neighborhood) level, we have here considered it to be uniform in the study area.

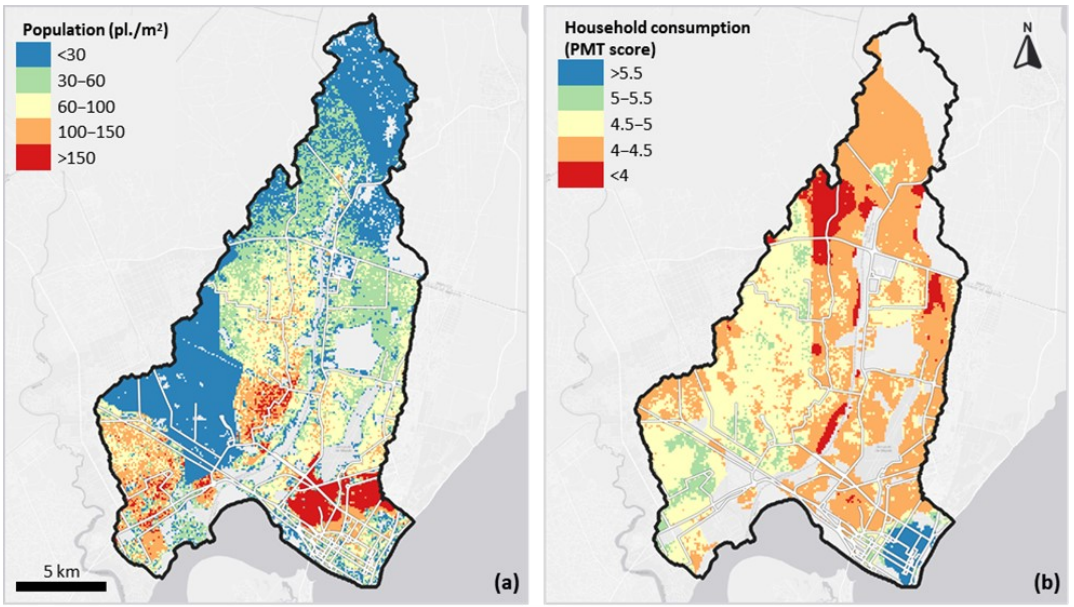

Fig. 4. (a) Exposure of human population (people per square meter) and map of (b) socioeconomic vulnerability in terms of poverty, based on the latest nationally representative household survey. Note that the PMT method makes use of observable characteristics of the household or its members to estimate their incomes or consumption, when other income data (salary slips, tax returns) are unavailable or unreliable. In this study, household income was determined based on questionnaires surveying: the household size, the number of children, the level of residents' education, the number of house rooms, the existence of water sanitation, connection to electricity grid, and possession of electronic devices.

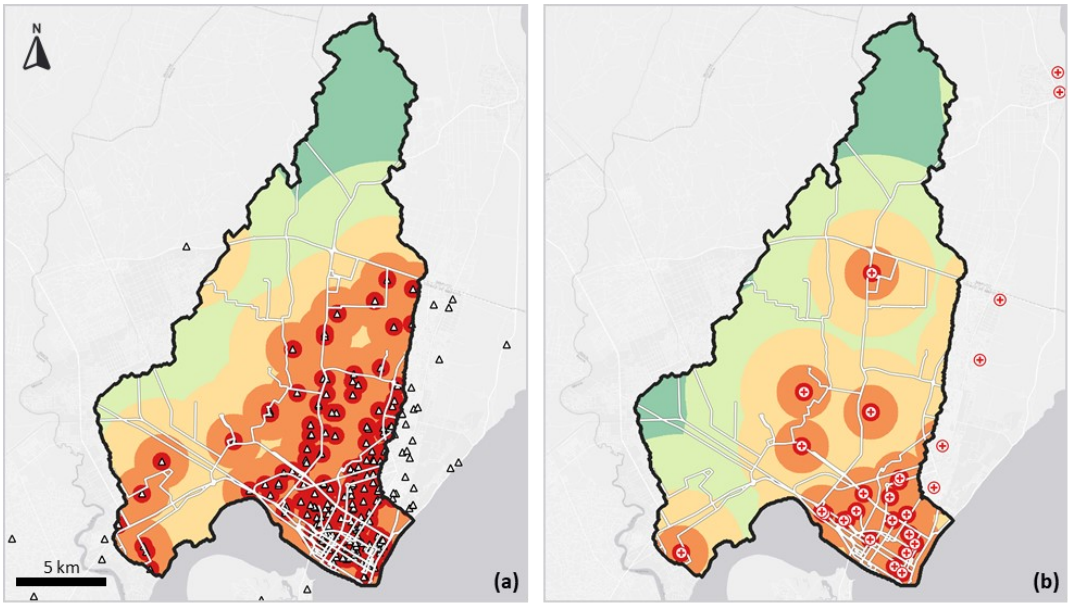

Fig. 5. Locations of critical facilities associated with aggregation of vulnerable groups (a) schools and (b) hospitals.

2.4. Risk

Figure 6 shows a map of the flood risk index in the study area calculated according to Equation (2) and classified in the same five categories as hazard:

$$R = (H\&E) \times V \times L \quad (2)$$

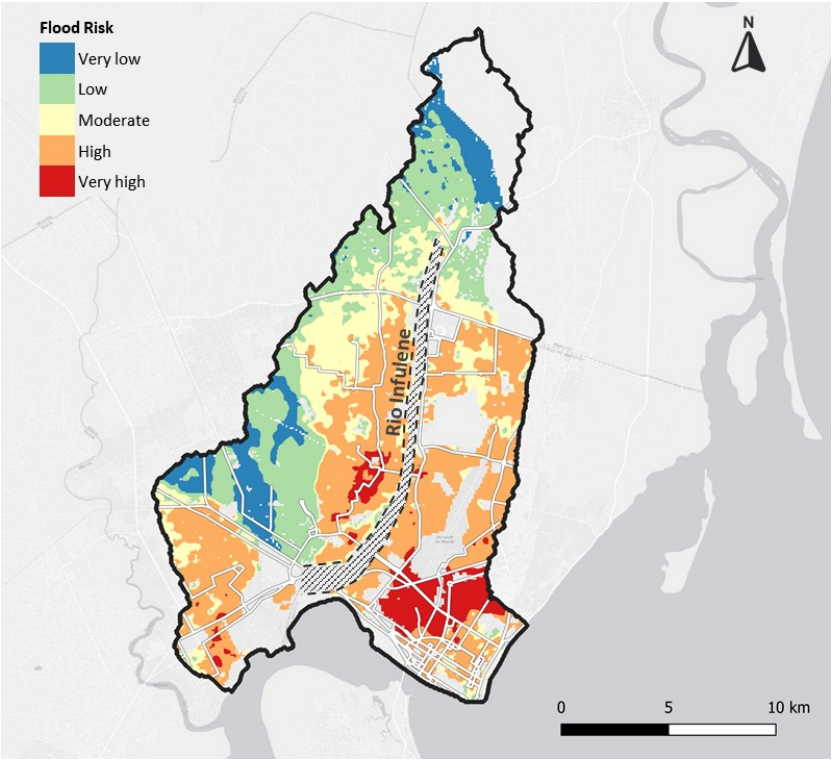

Fig. 6. Map of flood risk for the baseline (current climate) hazard scenario.

3. Conclusions

A GIS-based multi-criteria decision analysis of flood risk for road infrastructure in the metropolitan area of Maputo, Mozambique has considered socioeconomic drivers of vulnerability. The presented approach makes uses of a multitude of disparate datasets, including climatologic parameters, a new digital map of ground elevation appropriate for hydrologic analysis, the spatial distribution of the road network and of critical facilities associated with the presence of vulnerable groups, inventorying of historic floods in the region, and demographic data relevant to population density and poverty. We have mapped and classified present and future flood susceptibility at a regional level making use of climate change projections under SSP-5-8.5. Results indicate that segments of the primary and secondary road network amounting to a total length of 153 km are presently exposed to high or very high flood susceptibility. A 60% increase of this number would be expected by 2040, under pessimistic assumptions for climate and land-use change.

Through an integrated analysis that considers social vulnerabilities and the reduced capacity of vulnerable groups to cope with natural disasters, the paper presents a regional flood risk map that can be used to prioritize interventions for upgrading and adaptation of the road infrastructure (Loli, 2022) with the prospect to reduce inequalities and alleviate the marginalization and the vulnerability in Maputo's peri-urban communities. The framework presented can

be used as a benchmark to tackle similar challenges in developing countries in the face of natural disasters and sustained natural stressors due to climate change.

4. Limitations

The reader should bear in mind that the reported flood hazard indexing is qualitative in nature. Areas of low flood susceptibility (Fig. 3) are less likely to flood in comparison to high or very high susceptibility areas. Inundation of low susceptibility areas remains possible, depending on the hazard intensity.

Acknowledgements

The first author acknowledges funding by the European Union H2020-Marie Skłodowska-Curie Research Grants Scheme MSCA-IF-2019 (No. 895432: ReBounce).

The basis analysis was completed thanks to the generous funding provided by the Public-Private Infrastructure Advisory Facility (PPIAF) through its Climate Resilience & Environmental Sustainability Technical Advisory (CREST) initiative.

References

Arabameri, A., Rezaei, K., Cerdà, A., Conoscenti, C., & Kalantari, Z., 2019. A comparison of statistical methods and multi-criteria decision making to map flood hazard susceptibility in Northern Iran. Science of the Total Environment, 660, 443–458.

Bates, P. D., 2022. Flood Inundation Prediction. Annual Review of Fluid Mechanics, 54(1), 287–315.

Boyd, E., Ensor, J., Broto, V. C., & Juhola, S., 2014. Environmentalities of urban climate governance in Maputo, Mozambique. Global Environmental Change, 26, 140–151.

Cremen, G., Galasso, C., & McCloskey, J., 2022. Modelling and quantifying tomorrow's risks from natural hazards. Science of the Total Environment, 817, 152552.

Dodangeh, E., Choubin, B., Eigdir, A. N., Nabipour, N., Panahi, M., Shamshirband, S., & Mosavi, A., 2020. Integrated machine learning methods with resampling algorithms for flood susceptibility prediction. Science of the Total Environment, 705.

Hawker, L., Uhe, P., Paulo, L., Sosa, J., Savage, J., Sampson, C., & Neal, J., 2022. A 30 m global map of elevation with forests and buildings removed. Environmental Research Letters, 17(2), 024016.

Kapetas L., 2021. Updated GIS Map and Flood Risk Characterization and Recommendations. Technical Report, PPIAF, WB.

Kazakis, N., Kougias, I., & Patsialis, T. (2015). Assessment of flood hazard areas at a regional scale using an index-based approach and Analytical Hierarchy Process: Application in Rhodope-Evros region, Greece. Science of the Total Environment, 538, 555–563.

Loli, M., Mitoulis, S. M., Kefalas, G., Bouzoni, E., Kapetas L., Diaz-Fanas G., Arroyo Arroyo F. (2022). Flood risk for urban mobility in Maputo, Mozambique: Regional-scale indexing based on earth observation and demographic data. Proceedings of the 3rd International Conference on Natural Hazards and Infrastructure, ICONHIC2022, 5-7 July 2022, Athens, Greece.

Loli M., 2022. Recommendations of Climate Adaptation Measures for Flood Protection in MMA, Mozambique. Technical Report, PPIAF, WB.

Lyu, H. M., Sun, W. J., Shen, S. L., & Arulrajah, A. (2018). Flood risk assessment in metro systems of mega-cities using a GIS-based modeling approach. Science of the Total Environment, 626, 1012–1025. https://doi.org/10.1016/j.scitotenv.2018.01.138

Mahmoud, S. H., & Gan, T. Y. (2018). Urbanization and climate change implications in flood risk management: Developing an efficient decision support system for flood susceptibility mapping. Science of the Total Environment, 636, 152–167.

Marin-Ferrer, M., Vernaccini, L. and Poljansek, K., Index for Risk Management INFORM Concept and Methodology Report — Version 2017, EUR 28655 EN, doi:10.2760/094023

O'Neill, B. C., Tebaldi, C., Van Vuuren, D. P., Eyring, V., Friedlingstein, P., Hurtt, G., Knutti, R., Kriegler, E.,

Phongsapan, K., Chishtie, F., Poortinga, A., Bhandari, B., Meechaiya, C., Kunlamai, T., Aung, K. S., Saah, D., Anderson, E., Markert, K., Markert, A., & Towashiraporn, P. (2019). Operational Flood Risk Index Mapping for Disaster Risk Reduction Using Earth Observations and Cloud Computing Technologies: A Case Study on Myanmar. Frontiers in Environmental Science, 7(December), 1–15.

Sohnesen, T. P., Fisker, P., & Malmgren-Hansen, D. (2021). Using Satellite Data to Guide Urban Poverty Reduction. Review of Income and Wealth.

Tang, Z., Zhang, H., Yi, S., & Xiao, Y. (2018). Assessment of flood susceptible areas using spatially explicit, probabilistic multi-criteria decision analysis. Journal of Hydrology, 558, 144–158.

The World Bank (2022). Project Appraisal Document on a Proposed Grant in the Amount of US$ 250 million to the Republic of Mozambique for a Maputo Metropolitan Area Urban Mobility Project. International Development Association, pp. 89.

Wing, O. E. J., Lehman, W., Bates, P. D., Sampson, C. C., Quinn, N., Smith, A. M., Neal, J. C., Porter, J. R., & Kousky, C. (2022). Inequitable patterns of US flood risk in the Anthropocene. Nature Climate Change.